Effect of gamma irradiation dose on the structure and pH sensitivity of ITO thin films in extended gate field effect transistor

Amal Mohamed Ahmed Ali, Naser M. Ahmed, Sabah M. Mohammad, Fayroz A. Sabah, E.A. Kabaa, Ahmed Alsadig A, A.A. Sulieman

PII: S2211-3797(18)32387-8
DOI: https://doi.org/10.1016/j.rinp.2018.10.066
Reference: RINP 1769

To appear in: *Results in Physics*

Received Date: 5 October 2018
Revised Date: 30 October 2018
Accepted Date: 31 October 2018

Please cite this article as: Ahmed Ali, A.M., Ahmed, N.M., Mohammad, S.M., Sabah, F.A., Kabaa, E.A., Alsadig A, A., Sulieman, A.A., Effect of gamma irradiation dose on the structure and pH sensitivity of ITO thin films in extended gate field effect transistor, *Results in Physics* (2018), doi: https://doi.org/10.1016/j.rinp.2018.10.066

Effect of gamma irradiation dose on the structure and pH sensitivity of ITO thin films in extended gate field effect transistor

[1]Amal Mohamed Ahmed Ali, [2]Naser M. Ahmed , [3]Sabah M. Mohammad, [4]Fayroz A. Sabah, [5]E.A.Kabaa, [6]Ahmed Alsadig A, [7]A.A.Sulieman

[1,2,4,5]School of Physics, Universiti Sains Malaysia, 11800 Penang, Malaysia
[3]Institute of Nano Optoelectronics Research and Technology (INOR), Universiti Sains Malaysia, USM 11800, Penang, Malaysia
[6]Prince Sattam bin Abdulaziz University, Deanship of Preparatory Year, Alkharj, Saudi Arabia
[7]Prince Sattam bin Abdulaziz University, Collage of Applied Medical Sciences, Radiology and Medical Imaging Department, Alkharj, Saudi Arabia

ABSTRACT

Even though several studies have demonstrated the use ofIndium Tin Oxides (ITO) as an extended gate field effect transistor (EGFET), the effect of different doses of gamma radiation on the intrinsic properties of the ITO films has not been considered. This study investigates the effect of gamma irradiation on the structural, optical, morphological and electrical properties as well as pH sensitivity (as anextended gate field effect transistor) of ITO thin films. ITO thin films with thickness of 400 nm were prepared using a radio frequency sputtering technique. The samples were then subjected to various doses of gamma radiation from a Co-60 radio-isotope (0.5 kGy, 1 kGy, 1.5 kGy, and 2 kGy). The structural and morphological changes as well as transmission and absorption of the thin films were analyzed using X-ray diffraction (XRD), Atomic Force Microscopy (AFM), Field-Emission Scanning Electron Microscope (FESEM) and UV-Vis spectrophotometry, before and after irradiation. The irradiated ITO thin films were then used as an extended gate field effect transistor to determine its ability to improve sensitivity as pH sensors. The grain size and transmittance in the range 300-900 nm of the ITO films were found to decrease with increasing gamma irradiation dose. In contrast, the uniformity and surface roughness of ITO thin films increased with increasing gamma radiation dose due to the formation of lattice defects. Moreover, the electrical resistance of the thin films increased with increasing dose

because of the low current density and high number of surface defects associated with irradiation. The pH sensitivity of the ITO thin films improved after irradiation, possibly due to the concomitant increase in surface roughness with increasing radiation dose.The improvements in the pH sensitivity of ITO thin films after irradiation justifytheirpotential use as pH sensors.

Keywords: Indium Tin Oxide; Thin films; Gamma irradiation; Optical band gap; X-ray diffraction; EGFET; pH sensor.

1- Introduction

The phenomenon of thin films has been studied over the last three centuries. Moreover, metal oxide thin films have been widely applied in several fieldsover the last few decades due to their unique optical, electrical, mechanical, thermal and photochemicalproperties. For instance, thin films have been used as source materials for the manufacture of fuel cells, flat panel displays, solar cell, camera lenses and mirrors, gas sensors and biosensor, lasers and so on [1- 5].Furthermore, semiconductor materials such asthin films are known for their inherently high sensitivity to ionizing radiation, since their electrical, optical, structural and other physical propertiescan be altered byradiation. The interaction of gamma-rays with mattergenerally results in ionization and/or expulsion of atoms [14]. The influence of radiation depends on both radiation dose and synthesis parameters of thin films such as their thickness [15].

The transparent Indium Tin Oxide (ITO) thin film is specifically selected because of its intrinsic properties, which include transparency, high conductivity, and transmittance in the region between visible to infrared. In addition to being n-type,ITO is characterized by an energy band gap rangeof 3.2 eV - 4.2 eV. Furthermore, the deposition of ITO film involves

the generation of a huge concentration of oxygen vacancies and alternate tin dopants, which leads to increased conductivity of the film [6]. There are variousdeposition techniques for synthesizing ITO films, such as; chemical vapor deposition (CVD) [7], electron-beam evaporation [8], magnetron sputtering [9-10], pulsed laser deposition (PLD) [11-12] and spray pyrolysis [13].

On the other hand, the ion-sensitive field effect transistor (ISFET) is the foremost electrochemical sensor to use MOSFET. The ISFET was developed by Piet Bergveldin 1970 as a substitute for the Ion-sensitive electrode (ISE) [16].ISFET displayed smaller size, faster response time and mass setup compared to ISE[17]. Subsequently in 1983, J. Spiegel introduced the Extended Gate Field Effect Transistor (EGFET) as a replacement for ISFET [18]. EGFET was unique becauseof its ability to isolate the sensitive layer from the electronic components.Even thoughseveral studies have demonstrated the use of ITO as an extended gate field effect transistor (EGFET), the effect of different doses of gamma radiation on the optical, morphological and structural properties of the ITO films has not been considered. This is imperative given the ionization effect of radiation on semiconductor materials. Therefore, this study investigates the effect of gamma irradiation on the intrinsic properties and sensitivity of the thin film by measuring the pH sensitivity of deposited and irradiated ITO thin films.

2- Methodology

2.1 Preparation of the films

Sample preparation involved the deposition of 400 nm thick ITO thin films on glass substrates using Radio Frequency (RF) sputtering technique. The sputtering process was carried out with power of ~150W and pressure of ~ 3.16×10-3 mbar, and at a sputtering rate of 1.7 ÅS. The ITO films were kept at room temperature (~26 °C), and then exposed to

different doses of gamma radiation with a Co-60 source (0.5 kGy, 1 kGy, 1.5 kGy, and 2 kGy) by using gamma cell with an absorbed dose rate of 1.2 kGy/h at room temperature (~26 °C).

2.2 Characterization techniques

The structural properties of the deposited and irradiated ITO thin films were determined using the X-ray Diffractometer (X'Pert PRO, PANalytical) at2Θ range of 20^0 to 80^0.Based on the XRD data, the grain size (D) was calculated using the Scherer's formula[19], expressed below (Eq. 1).

$$\mathbf{D}=\frac{\mathbf{0.89}\,\boldsymbol{\lambda}}{\boldsymbol{B}\,\boldsymbol{cos\theta_B}} \quad (1)$$

Where B denotes the full width at half maximum (FWHM) of the XRD peaks, $\theta_B$symbolizes the Bragg diffraction angle, and λ signifies the X-ray wavelength (0.154nm). FESEM was used to morphologically characterize the samples. AFM machine (edge, BRUKER) was employedformorphological and surface roughness characterizations of the ITO thin films before and after exposure to radiation. Ultraviolet-visible spectroscopy (UV-Vis) was used to evaluate the transmission and absorption in thewavelength range of 300 - 900 nm and 200 - 900 nm, respectively.The energy gap (***Eg***) was determinedthrough the calculation of absorption coefficient (α) from the equation below (Eq. 2):

$$\boldsymbol{\alpha} = (\mathbf{1}/\boldsymbol{d})\mathbf{ln}\,(\mathbf{1} - \boldsymbol{A}/\mathbf{10}) \quad (2)$$

Where ***d***and ***A***denotes the thickness andabsorption of the film, respectively. The band gap was calculated using the followingTauc's equation (Eq. 3):

$$\boldsymbol{\alpha h\nu = A(h\nu - E_g)^n} \quad (3)$$

Where Asignifies a constant and $E_g$denotes the band gap of the material, n = 1/2, 2, 3, 3/2 for direct allowed, indirect allowed, indirect forbidden and direct forbidden transitions, respectively. Thus, the "n" value is dependent on thetransition type. The present system follows the rule of direct transition (i.e., n = 1/2).

2.3 EGFET pH sensor setup and measurement

The Keithley Semiconductor Characterization System (2400-SCS) was used to determine the pH sensitivity of deposited and irradiated ITO thin films. The EGFET pH sensor setup comprises a PC, Keithley, MOSFET, cavity, a reference electrode and buffer solutions (pH 2, pH 4, pH 6, pH 8, pH 10 and pH 12).

The ITO thin films were used as sensing membrane for EGFET of pH sensor. The thin films were connected to MOSFET gate butplaced far from the transistor. First, the deposited ITO thin films were immersed in the buffer solution of pH 2.The (I_{ds}–V_{ds}) and (I_{ds}–V_{gs}) curves for saturation and linear regimes were then plotted. The measuring process started by applying 3 V to Vgs and Vds would sweep the range (0 - 5) V in the saturation regime. While in the linear regime, Vds would be fixed (0.3) V and Vgs would sweep the range (0 - 3.5) V. These steps were repeated for pH solution 4, 6, 8, 10 and 12 for all irradiated samples. From the (I-V) curves for each regime separately, one point must be selected on the (current-axis) and (voltage-axis) per each regime curve. For the saturation regime, a saturated point in the x-axis (voltage) will be selected to obtain the current values for all pH values. Also, for the linear regime (one point in the linear region of current will be selected to get the voltage values for all pH values). Then the pH sensitivity of the films was determined from the slope by plotting (I–pH value) and (V-pH value) curves. The pH sensitivity values of the films were then determined from the slopes of (I–pH value) and (V-pH value) curves [20]. These steps were repeated for solutions of pH 4, pH6, pH8, pH10 and pH12 for all irradiated samples.

3- Results and discussion

3.1. Structural properties of ITO thin films

3.1.1 XRD results of ITO thin films

X-ray diffraction (XRD) measurements were used to determine the phase structure and calculate the grain size of irradiated ITO thin films. The XRD spectra of as-deposited thin films,and films exposed to gamma irradiation of 0 kGy, 0.5 kGy, 1 kGy, 1.5 kGy, and 2 kGy are shown in Figure 1.The (211), (222), (431) and (440) crystallite peaks were identified for ITO. The highest intensity and most distinctdiffraction peak appeared at $51^0$with (440)orientation, while the second highest intensitypeak (222) emerged at 30.5^0.It was observed that the intensity of diffraction peak at 51^0 decreased with increasing irradiation dose, while that of the diffraction peak at 30.5^0increased. Furthermore, a new diffraction peak emerged at 25.5° as the irradiation dose increased. The grain sizes of the ITO thin films were then calculated using Eq. 3. The grain size decreased with increasing irradiation dose as following 62.59 nm, 62.58nm, 31.21nm, and then to 16.09 nm for doses 0, 0.5, 1, and 1.5 kGy, respectively. Followed by a rebound to 62.6 nm at 2 kGy. This decrease in grain size with increasing irradiation can be attributed to the ionization of the thin films by gamma irradiation [21]. However, the riseand rebound in grain size with further increase in irradiation dose from1.5 kGyto 2kGy can be attributed to the decreased value of dislocation density asthe gamma irradiationis increased beyond 1.5 kGy, which leads to crystal growth of the ITO material [21-23]. Therefore, changes in the atomic arrangement can also be associated with gamma dose [24].

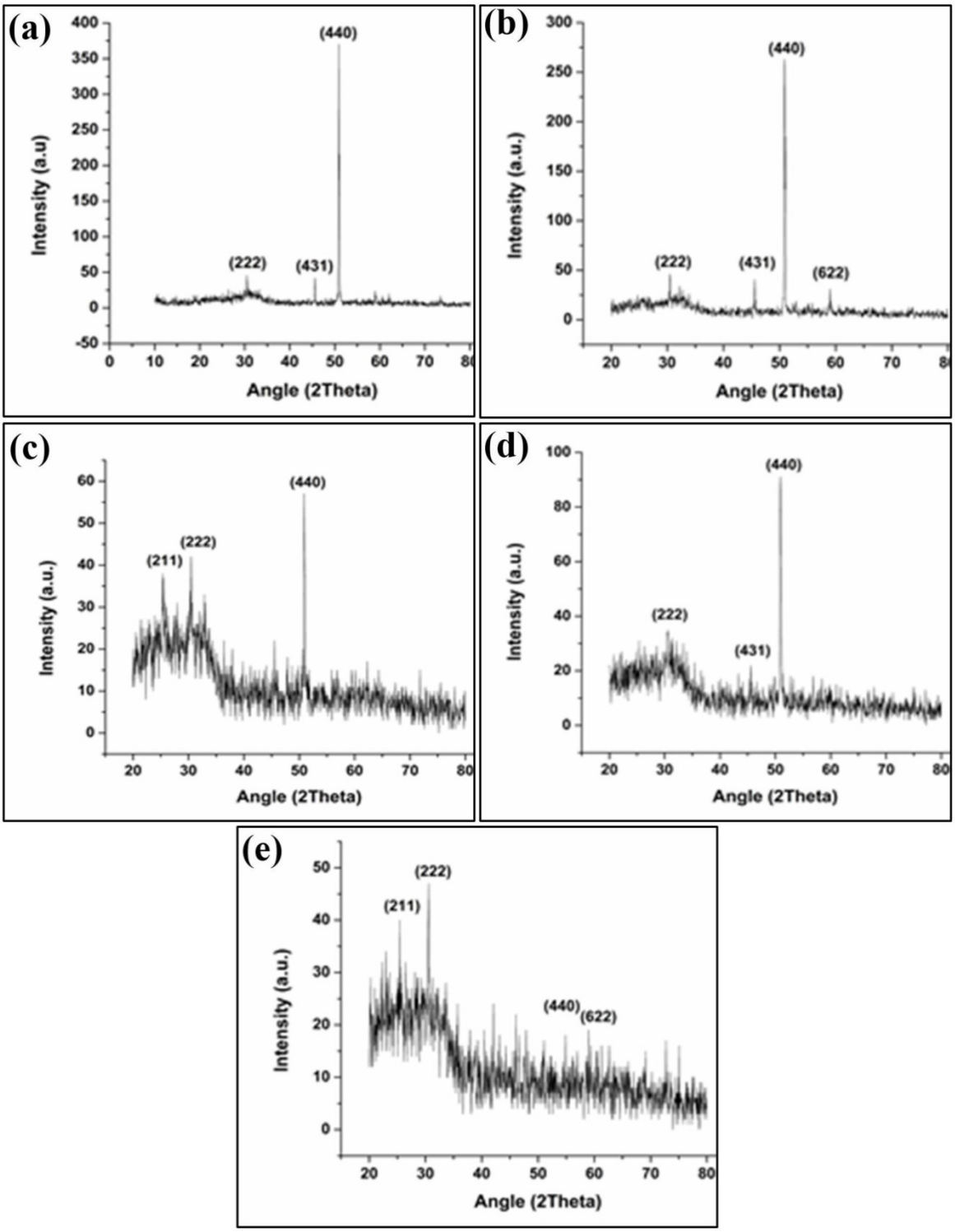

Figure 1: (a-e)the XRD patterns of 0 kGy, 0.5 kGy, 1 kGy, 1.5 kGy and 2 kGy, respectively.

3.1.2 FESEM results of ITO thin film

The FESEM images obtained for 400 nm thick ITO thin films exposed to different doses of gamma radiation are shown inFigure 2. As observed, the uniformity and clustering of grains increased withincreasing gamma irradiation. Distinct voids emerge in the thin film exposedto the highest radiation dose.Theclusters and voids can be attributed to the advent of defects (i.e.structural disorders), which form when gamma radiation interacts with the film [25].

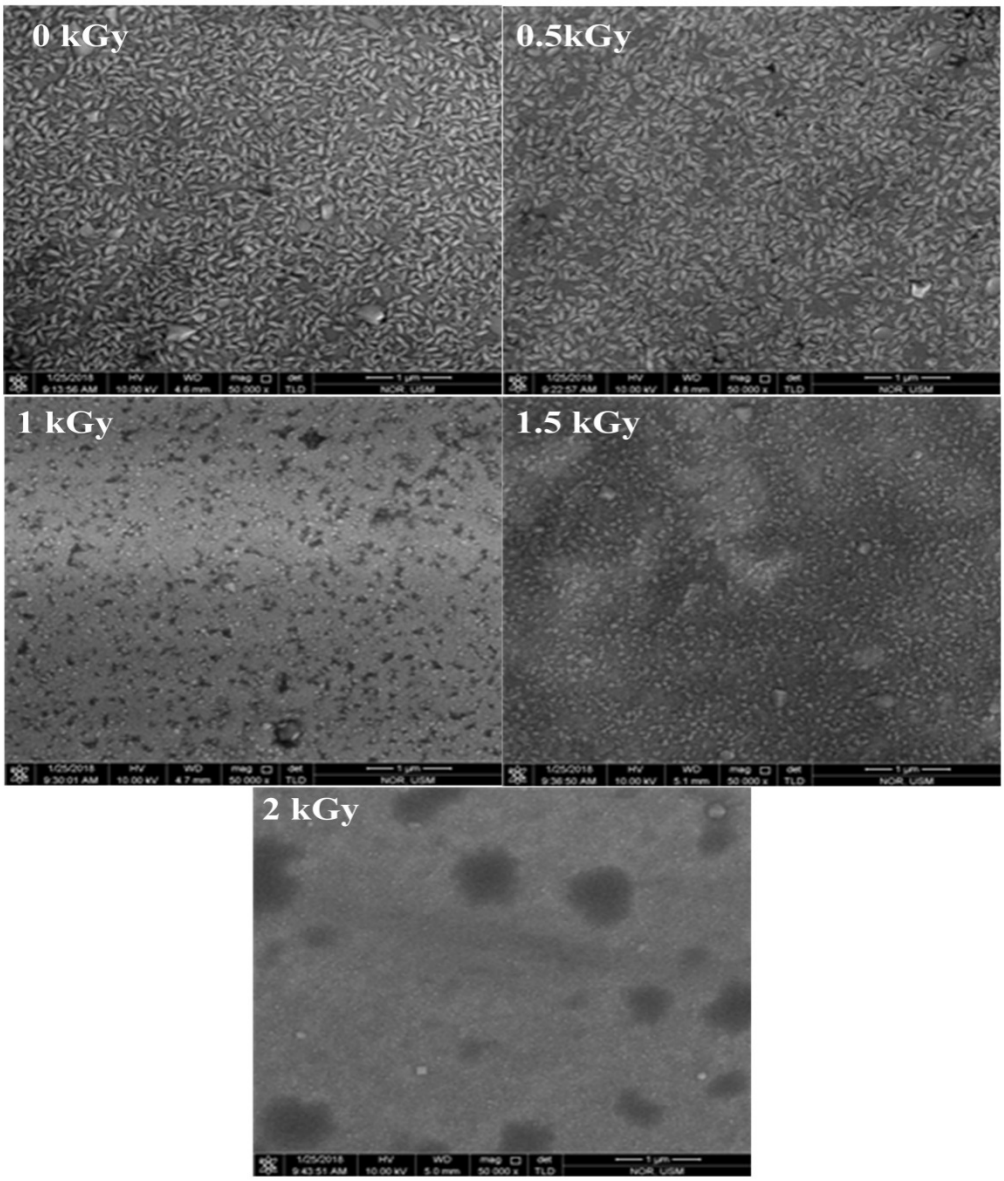

Figure 2(a-e): FESEM image for deposited and irradiated ITO thin films.

3.2 Optical properties of ITO thin films

The transmittance spectra of the deposited and irradiatedITO films were obtainedin the region of 300 nm - 900 nm. As observed in Figure 3, the transmittance of the ITO films has decreased from ~ 87% for the deposited film (0 kGy) to ~ 75% for the film exposed to radiation dose of 2 kGy. The reduction in transmittance with increasing radiation exposure is due to: increase in vacancy defects, which simultaneously leads to increase in absorption [15] and the concomitant increase in carrier density withincrease in the ratio of metal to oxygen[26].

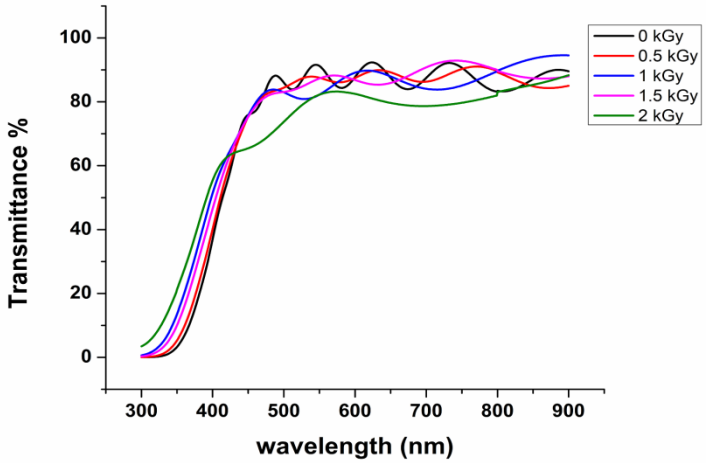

Figure 3: Transmittance of the deposited and irradiated thin films.

The energy gap (Eg) was determined using Eqn. (1) and (2). The energy band gap was obtained from the plot of $(\alpha h\nu)^2$(y-axis)againsthy(x-axis) by extrapolating a straight portion on the x-axis, as shown in Figure 4. It was deduced that as the gamma irradiation dose increases,the value of optical band gap increases from 2.86 eV for the deposited film (0 kGy) to 2.91 eV for the film exposed to 1.5 kGy, followed by a subsequent decrease to 2.83eVas the dose increases to 2 kGy. This increase in energy gap with radiation dose is attributed to the high structural disorder created at high radiation dose [25]. The subsequent decline in

band gap is attributed to the rise in the width of the energy of the band tails of localized states, which is consistent withrelated studies by other researchers [25, 27-28].

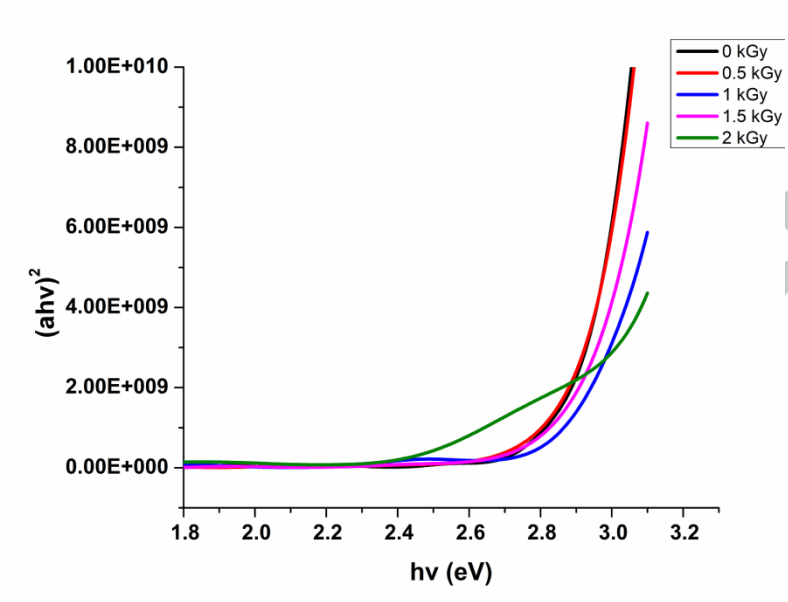

Figure 4: the Tauc's plot of as-deposited and irradiated ITO thin films.

3.4 Morphology of ITO thin films

AFM was utilized to characterize the morphological variations and surface roughness of the non-irradiated and irradiated ITO films. Figure 5shows the AFM imagesof the ITO thin films and their corresponding three-dimensional images. The surface roughness increased from 9.26 nm for as-depositedthin films to 15.9 nm for samples exposed to radiation dose of 0.5 kGy. The surface roughnessthen increased drasticallyto 20.10 nm for the highest dose (2 kGy).The different absorbed radiation dosesresulted in the formation of different surface textures and roughness. It can be concluded from the 3-D images that surface roughness isdirectly proportional to the dose of irradiation exposure.

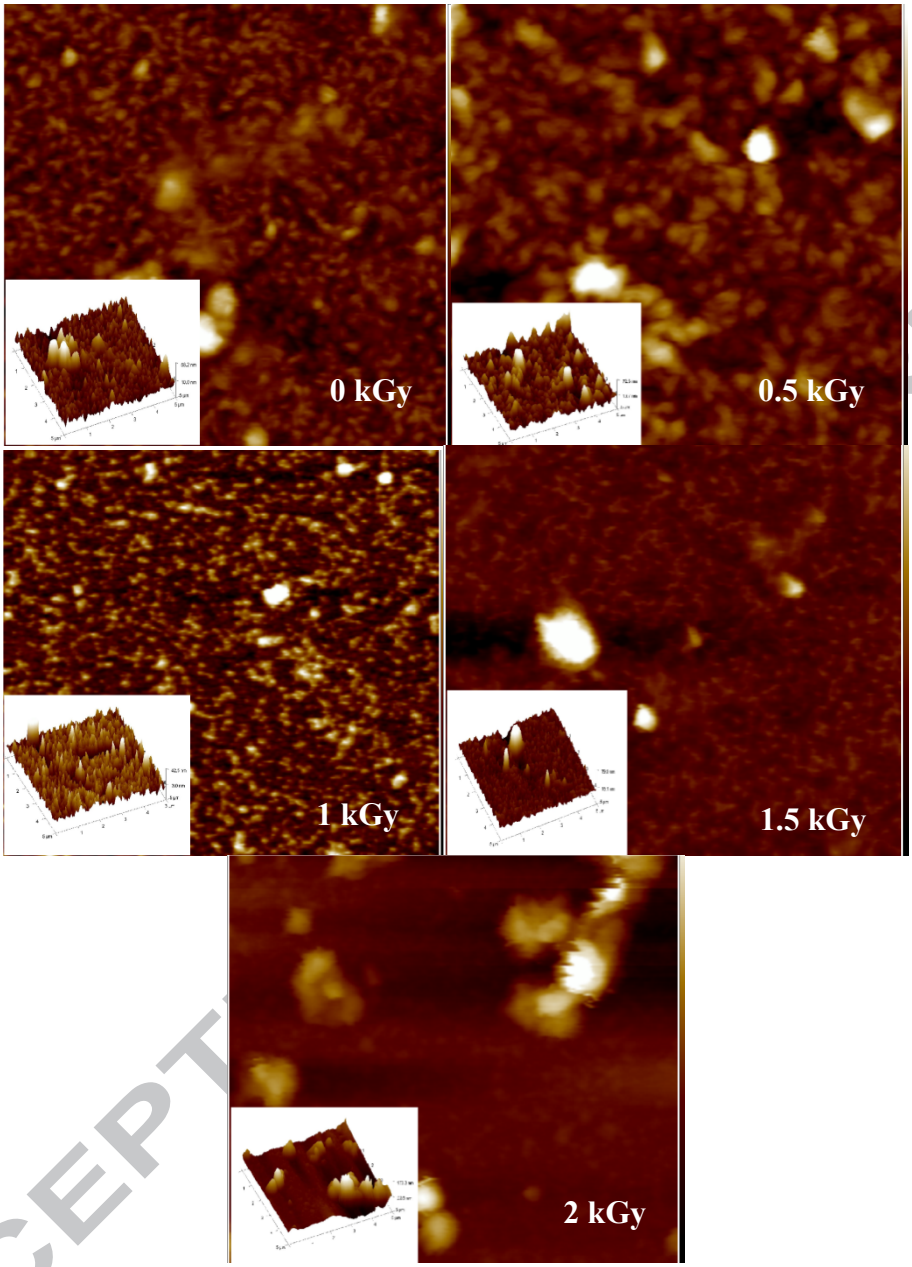

Figure 5: the AFM images of deposited and irradiated ITO thin films with different dose.

3.3 Electrical properties of ITO thin film

The electrical resistance of the irradiated ITO thin films increased considerably by more than two fold as the radiation dose increased from 1.5 kGy to 2 kGy. This increase in resistance could be due to the decreased current density and elevated number of defects that are associated with increasing radiation dose [25].

3.5 Study of the pH sensitivity

The curves for saturation and linear regimes of deposited and irradiated ITO thin films are shown in Figure 6 and Figure 7, respectively, under variable pH values (2, 4, 6, 8, 10 and 12). The sensitivity values of the deposited and irradiated ITO thin films were calculated by plotting (I–pH value) and (V-pH value) curves. The current decreased with increasing pH in the saturation regime, while the voltage increased with increasing pH in the linear regime for both deposited and irradiated ITO thin films. The voltage and current sensitivities of the deposited ITO thin film were 39.8 µA/pH and 38.3 mV/pH, in both saturation and linear regimes, respectively as observed in Figure 8. The current and voltage sensitivities of irradiated ITO thin films derived from the slope were 30.5 µA/pH; 34 mV/pH, 63.8 µA/pH; 71.3 mV/pH, 107.2 µA/pH; 89.7 mV/pH and 102.4 µA/pH; 79.8 mV/pH for 0.5 kGy, 1 kGy. 1.5 kGy and 2 kGy, respectively, as shown in Figure 9. Therefore, the pH sensitivity improved with increase in both gamma radiation dose and surface roughness [29-30]. The sensitivity values of the as-deposited and irradiated ITO thin films are presented in Table 1.

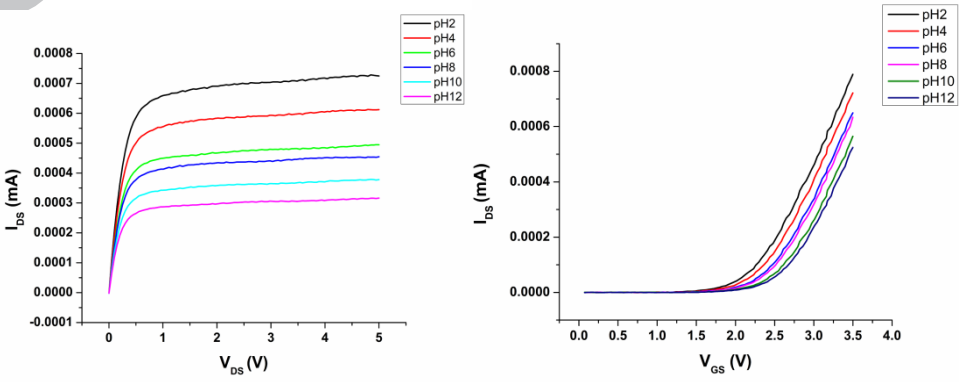

Figure 6: (I_{ds}–V_{ds}) and (I_{ds}–V_{gs}) curves for saturation and linear regimes of deposited ITO thin film.

(a)

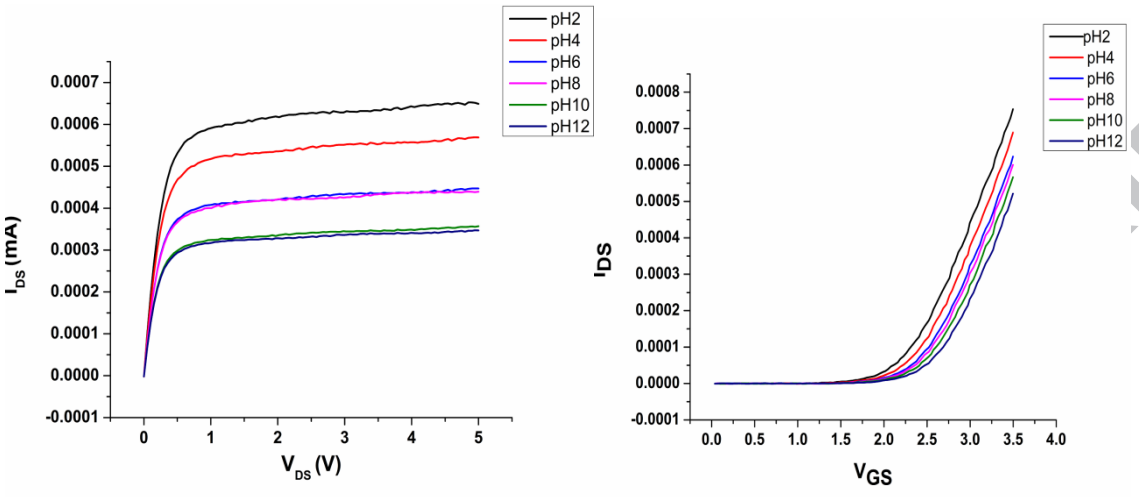

(b)

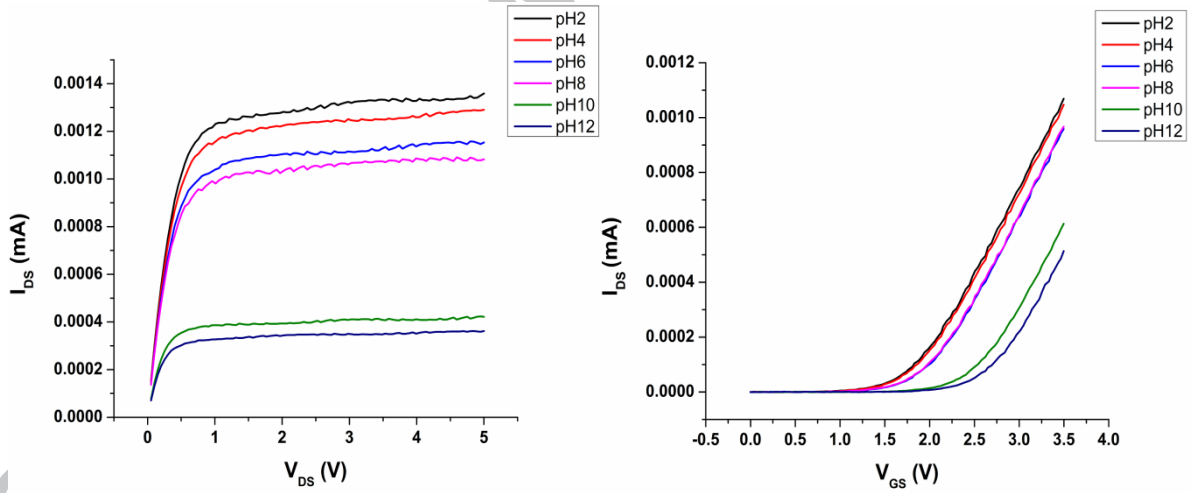

(c)

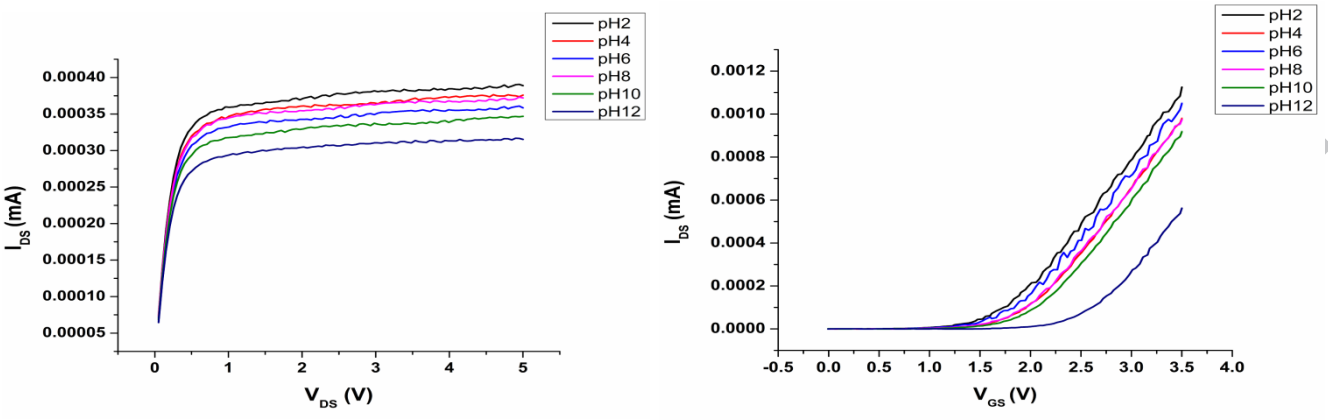

(d)

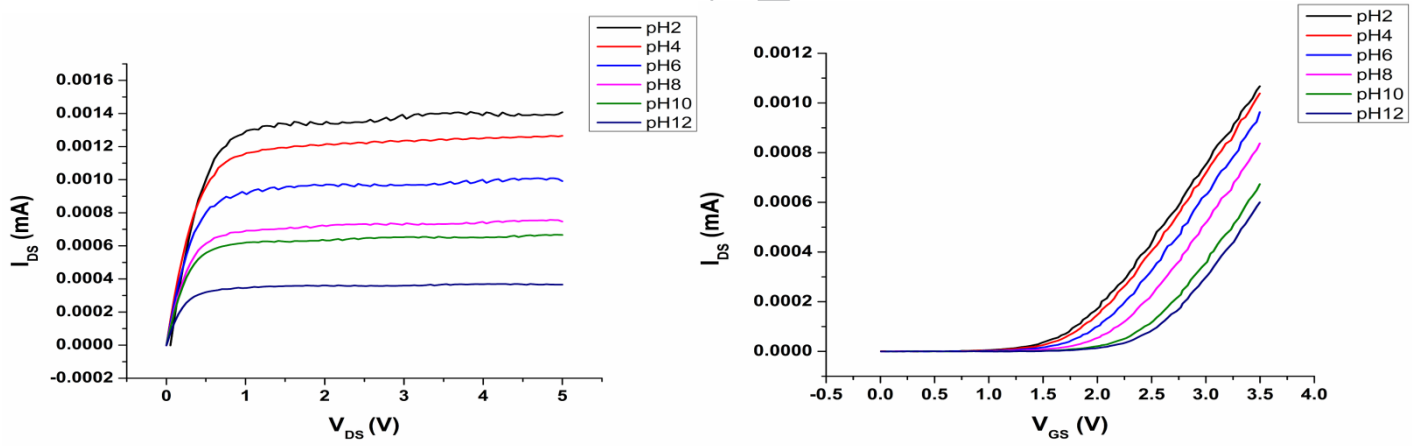

Figure 7: (a-d); illustrates (Ids–Vds) and (Ids–Vgs) curves for saturation and linear regimes of irradiated ITO thin films; (a) 0.5 kGy, (b) 1 kGy, (c) 1.5 kGy and (d) 2 kGy.

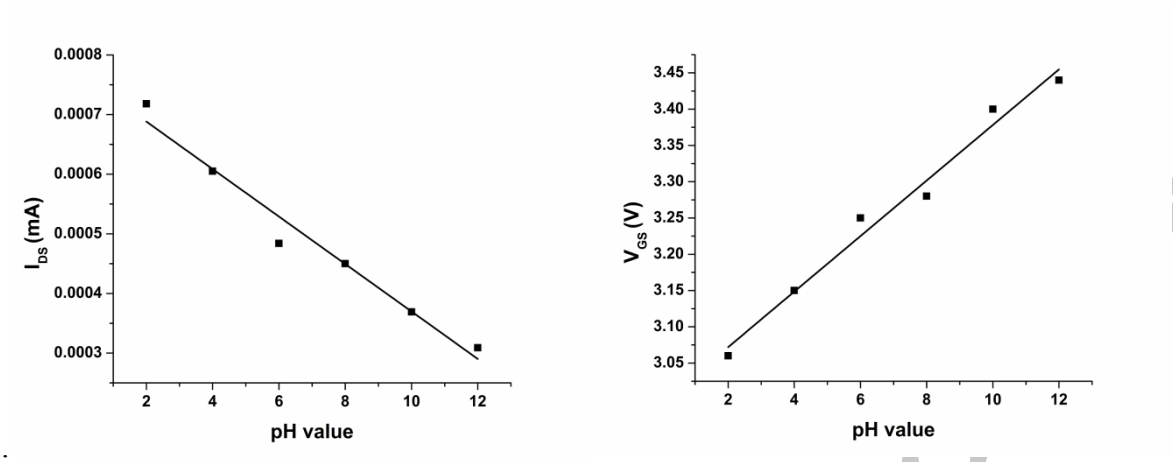

Figure 8: The current and voltage sensitivities of as-deposited ITO thin film.

(a)

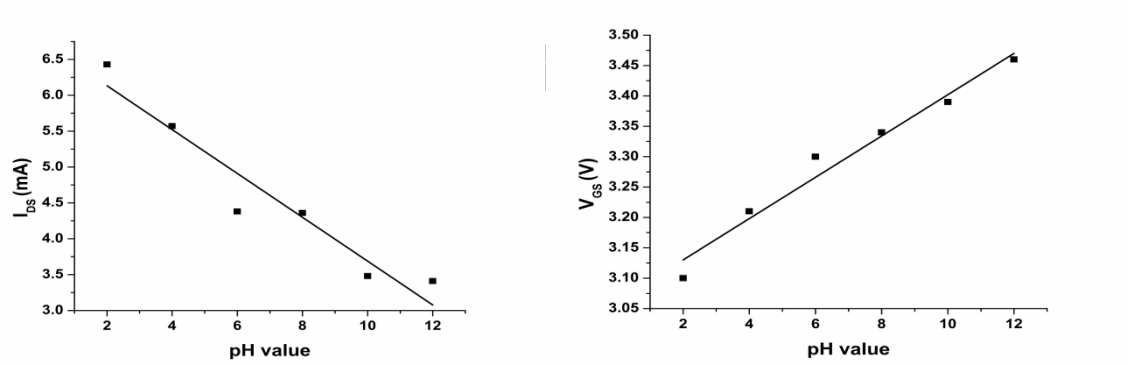

(b)

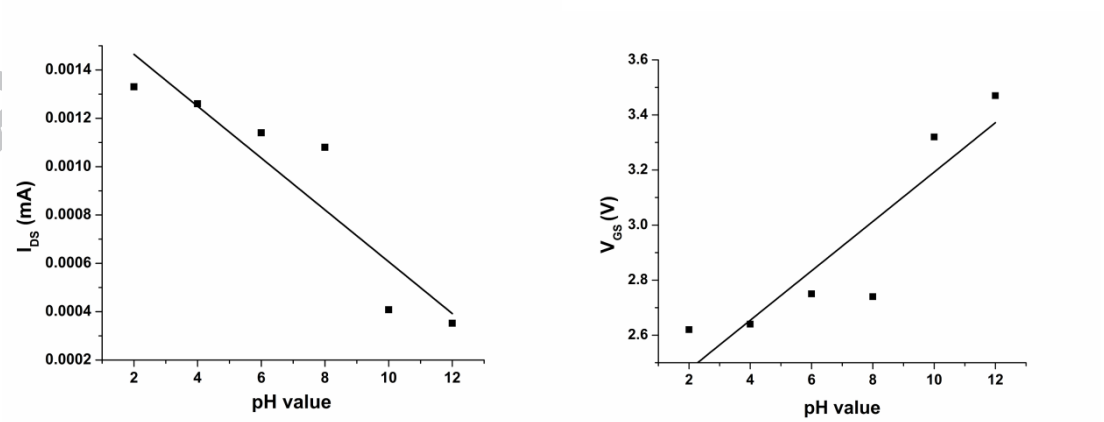

(c)

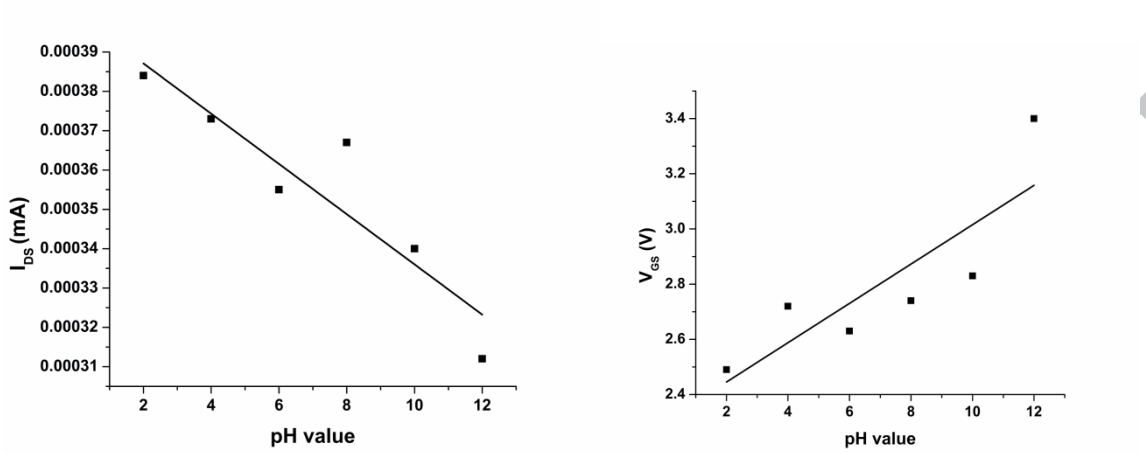

(d)

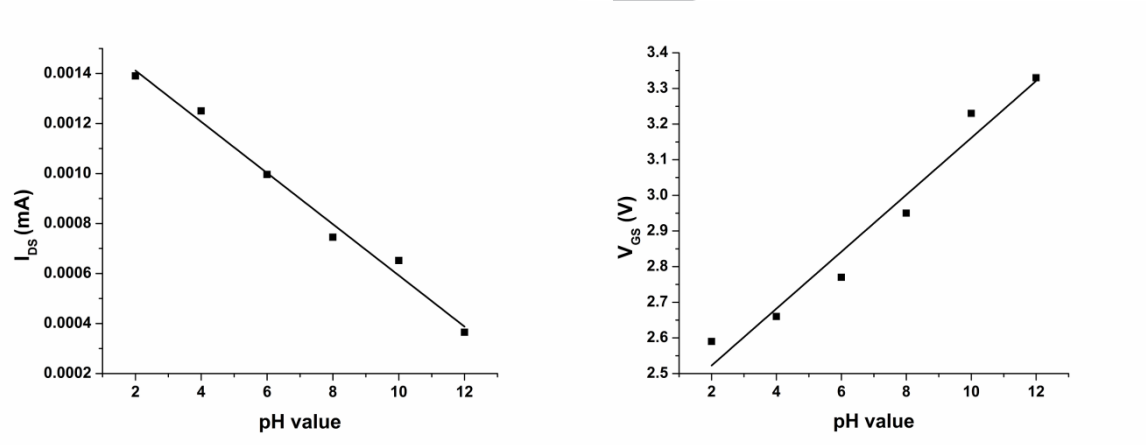

Figure 9: Figure 9 (a-d): The current and voltage sensitivities of irradiated ITO thin films; (a) 0.5 kGy, (b) 1 kGy, (c) 1.5 kGy and (d) 2 kGy.

Table 1: summary of the resistance, roughness, transmission, energy gap, grain size and pH sensitivity of the as-deposited and irradiated ITO films.

Dose (kGy)	Resistance (Ω)	Roughness (nm)	Transmission %		Energy gap (eV)	Grain size (nm)		pH sensitivity	
			500 nm	700 nm		At 30°	At 50°	Linear (mV/pH)	Saturation (µA/pH)
0	135	9.26	86.00	87.31	2.86	62.59	64.09	38.3	39.8
0.5	457	15.9	84.42	86.30	2.88	62.58	64.08	34.0	30.5
1	1660	7.94	83.00	84.03	2.89	31.21	51.22	71.29	63.8
1.5	3800	10.40	83.08	90.84	2.91	16.09	64.12	89.7	107.2
2	5750	20.10	73.74	78.61	2.83	62.60	80.45	79.8	102.4

.

4- Conclusion

This study investigated the effect of gamma irradiation on thestructural, optical, morphological and electrical properties as well as pH sensitivity of ITO thin films prepared using the radio frequency (RF) sputtering technique. XRD showed thatdiffraction peak intensity and grain size decreased with increasing dose of gamma radiation. Surface characterization using FESEM and AFM showed improved uniformityand thedevelopment of voidsdue to the formation of defects in the film after irradiation. The transmittance in the range 300-900 nm of ITO films slightly decreased with increasing gamma irradiation dose, which isattributable to the advent of lattice defects.In contrast, the surface roughness of ITO thin films increased with increasing gamma radiation dose. Moreover, the electrical resistance of the thin films increased with increasing dose because of the low current density and high number of surface defects associated with irradiation.The pH sensitivity of theITO thin films improved after irradiation, possibly due to the concomitant increase in surface

roughness with increasing radiation dose.The improvement in the pH sensitivity of ITO thin films after irradiation justifies their potential use as pH sensors.

5- Acknowledgement:

The authors wish to express their sincere gratitude to the School of Physics, UniversitiSains Malaysia together with mix-mode final project Incentive Grant for the tremendous support.

References

[1]Wang, H. T., Kang, B. S., Ren, F., Tien, L. C., Sadik, P. W., Norton, D. P. & Lin, J. (2005). *Appl. Phys. Lett.*, **86(**24), 243503.

[2] H.K. Yu, J.M. Baik, J.-L. Lee,(2011)*Cryst. Growth Des*. **11** (6) 2438.

[3] S.K. Park, J. In Han, W.K. Kim, M. GiKwak, (2001).*Thin Solid Films***397** (1–2) 49.

[4] Patel, N. G., Patel, P. D., & Vaishnav, V. S. (2003). *Sens. Actuator B-Chem.*, **96**(1-2), 180.

[5] Chen, M. F., Lin, K. M., & Ho, Y. S. (2012). *Opt. Lasers Eng.***50**(3), 491.

[6] Løvvik, O. M., Diplas, S., Romanyuk, A., &Ulyashin, A. (2014). *J. Appl. Phys.***115**(8), 083705.

[7] Maruyama, T., & Fukui, K. (1991). *Thin solid films*, **203**(2), 297.

[8] Ishida, T., Kobayashi, H., &Nakato, Y. (1993). *J. Appl. Phys.***73**(9), 4344.

[9] Wu, W. F., Chiou, B. S., & Hsieh, S. T. (1994). *Semicond. Sci. Technol*. **9**(6), 1242.

[10] Buchanan, M., Webb, J. B., & Williams, D. F. (1980). *Appl. Phys. Lett.*, **37**(2), 213.

[11] Kim, H., Pique, A., Horwitz, J. S., Murata, H., Kafafi, Z. H., Gilmore, C. M., &Chrisey, D. B. (2000). *Thin solid films*, **377**, 798.

[12] Morales-Paliza, M. A., Haglund Jr, R. F., & Feldman, L. C. (2002). *Appl. Phys. Lett.*, **80**(20), 3757.

[13] Vasu, V., & Subrahmanyam, A. (1990). Thin Solid Films, **193**, 696.

[14]Chen, C. H., Talnagi, J., Liu, J., Vora, P., Higgins, A., & Liu, S. (2005). *IEEE Trans. Magn.,* **41**(10), 3832.

[15] Alyamani, A., & Mustapha, N. (2016). *Thin Solid Films*, **611**, 27.

[16Bausells, J., Carrabina, J., Errachid, A., &Merlos, A. (1999). *Sens. Actuator B-Chem.*, **57**(1-3), 56.

[17] Chou, J. L. C. J. C., & Chen, Y. C. (2001). *J. Med. Biol. Eng.*, **21**(3), 135.

[18] Lauks, I., Chan, P., &Babic, D. (1983). *Sens. Actuator*, **4**, 291.

[19] Paufler, P.. CS Barrett, TB Massalski. (1981). *Cryst. Res. Technol.*, **16**(9), 982.

[20] Sabah, F. A., Ahmed, N. M., Hassan, Z., & Al-Hardan, N. H. (2016). *Appl. Phys. A*, **122**(9), 839.

[21] El-Shobaky, G. A., El-Shaabiny, A. M., Ramadan, A. A., &Dessouki, A. M. (1989). *Radiat. Phys. Chem*, **34**, 787.

[22] Ahmad, S., Asokan, K., Khan, M. S., &Zulfequar, M. (2015). *Radiat. Eff. Defects Solids.*, **170**(12), 956.

[23] Williamson, G. K., & Smallman, R. E. (1956). *Philos. Mag.,***1**(1), 34.

[24] Padiyan, D. P., Marikani, A., & Murali, K. R. (2003). *Mater. Chem. Phys.,***78**(1), 51.

[25] Maity, T. K., & Sharma, S. L. (2011). *NISCAIR-CSIR*, **49**(09), 606.

[26] Mohil, M., & Kumar, G. A. (2013). *J. Nano- Electron. Phys.,* **5**(2), 2018.

[27] Sharma, S. L., &Maity, T. K. (2011). *B Mater Sci.*, **34**(1), 61.

[28] Alwan, T. J. (2012).*Turk J Phys*, **36**(3), 377.

[29] Pan, T. M., Lin, J. C., Wu, M. H., & Lai, C. S. (2009). *Biosens. Bioelectron.*, **24**(9), 2864.

[30] Wu, M. H., Cheng, C. H., Lai, C. S., & Pan, T. M. (2009). *Sens. Actuator B-Chem.*, **138**(1), 221.

List of figure captions

Figure 1 (a-e): the XRD patterns of as-deposited, 0 kGy, 0.5 kGy, 1 kGy, 1.5 kGy and 2 kGy, respectively.

Figure 2 (a-e): FESEM image for as-deposited and irradiated ITO thin film.

Figure 3: the transmittance of the as-deposited and irradiated thin films.

Figure 4: the Tauc's plot of as-deposited and irradiated ITO thin films.

Figure 5 (a-e): the AFM images and their corresponding 3-dimensional images of as-deposited and irradiated ITO thin films.

Figure 6: (Ids–Vds) and (Ids–Vgs) curves for saturation and linear regimes of as-deposited ITO thin film.

Figure 7 (a-d); illustrates (Ids–Vds) and (Ids–Vgs) curves for saturation and linear regimes of irradiated ITO thin films; (a) 0.5 kGy, (b) 1 kGy, (c) 1.5 kGy and (d) 2 kGy.

Figure 8: The current sensitivity and voltage sensitivity of as-deposited ITO thin film.

Figure 9 (a-d): The current sensitivity and voltage sensitivity of irradiated ITO thin films; (a) 0.5 kGy, (b) 1 kGy, (c) 1.5 kGy and (d) 2 kGy.

List of table captions

Table 1; summary of the resistance, roughness, transmission, energy gap, grain size and pH sensitivity of the as-deposited and irradiated ITO films.